

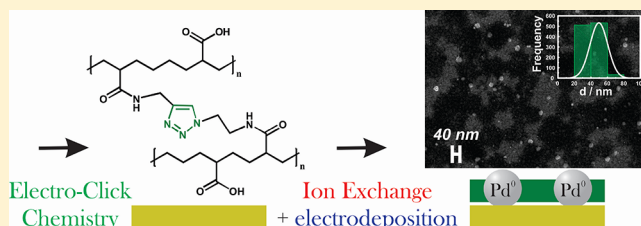
Palladium Nanoparticles Embedded in a Layer-by-Layer Nanoreactor Built with Poly(Acrylic Acid) Using “Electro-Click Chemistry”

Matias Villalba, Mariano Bossi, Maria del Pozo, and Ernesto J. Calvo*

INQUIMAE, Facultad de Ciencias Exactas y Naturales, Universidad de Buenos Aires, Pabellon 2, Ciudad Universitaria, AR-1428 Buenos Aires, Argentina

Supporting Information

ABSTRACT: Palladium nanoparticles (Pd NPs) were formed by electrochemical reduction of $\text{Pd}(\text{NH}_3)_4^{3+}$ ions entrapped by ion exchange in poly(acrylic acid) (PAA) multilayer films grown by the Sharpless “click reaction.” The alkyne (PAA_{alk}) and azide (PAA_{az}) groups were covalently bound to the PAA, and the catalyzed buildup of the multilayer film was performed by electrochemical reduction of Cu^{2+} to Cu^+ . The size of the Pd NPs formed in $\text{Au}/(\text{PAA}_{\text{alk}})_3(\text{PAA}_{\text{az}})_2$ multilayer films by the click reaction, that is, 50 nm, is larger than that of similar Pd NPs formed in electrostatically bound $\text{Au}/(\text{PAA})_3(\text{PAH})_2$ nanoreactors, that is, 6–9 nm, under similar conditions. A combination of electrochemical methods and electrochemical quartz crystal microbalance, polarization modulation infrared reflection absorption spectroscopy (PM-IRRAS), ellipsometry, and scanning electron microscopy has been used to follow these processes. Cyclic voltammetry of the resulting Pd NPs in a 0.1 M H_2SO_4 solution at $0.1 \text{ V} \cdot \text{s}^{-1}$ shows the PdO reduction peak at the same potential as that on the clean Pd surface unlike the NPs formed in electrostatically self-assembled $\text{Au}/(\text{PAA})_3(\text{PAH})_2$ nanoreactors with a 0.2 V shift in the cathodic direction most probably because of the strong adsorption of amino groups on the Pd NP surfaces.



INTRODUCTION

Polyelectrolyte multilayer (PEM) films formed by the layer-by-layer (LbL) adsorption of oppositely charged polyelectrolytes^{1,2} are easy to build³ and lead to robust thin films with tunable architectures. An interesting application is the use of PEM films for the “in situ” preparation of metal nanoparticles (NPs).^{4,5}

Rubner, Cohen, and co-workers^{6,7} described the growth of metal NPs from coordinated metal ions in LbL PEM films as nanoreactors. Electrostatically self-assembled multilayers were immersed in solutions containing the respective cations Ag^+ , Pb^{2+} , or $\text{Pd}(\text{NH}_3)_4^{2+}$, which bind to carboxylic groups in poly(acrylic acid) (PAA) and, subsequently, the ion-exchanged cations were converted to NPs by chemical reduction or sulfidation. Kidambi and Bruening^{8–10} have developed an alternative method in which palladium (Pd) ions were codeposited during the multilayer formation, and the system was applied to selective hydrogenation catalysis. Vago and co-workers¹¹ described a highly efficient and selective material for electrocatalytic hydrogenation prepared by electrochemical reduction of PdCl_4^{2-} confined in a poly(allyl amines)/PAA PEM nanostructure yielding $6 \pm 1 \text{ nm}$ Pd NPs. This work demonstrated for the first time that homogeneous metal NPs can be formed within PEM films by direct electrochemical reduction.

Villalba et al.¹² have recently reported that confining PdCl_4^{2-} ions in self-assembled $(\text{PAH})_n(\text{PAA})_m$ PEMs not only prevents the formation of large crystals upon electrochemical reduction but also the presence of polyelectrolytes affects hydrogenation

and the PdO reduction reactions. However, after heat-treatment elimination of free amino groups, which are adsorbed on Pd surfaces, the Pd NPs recover the electrochemical behavior of pure Pd electrodes.

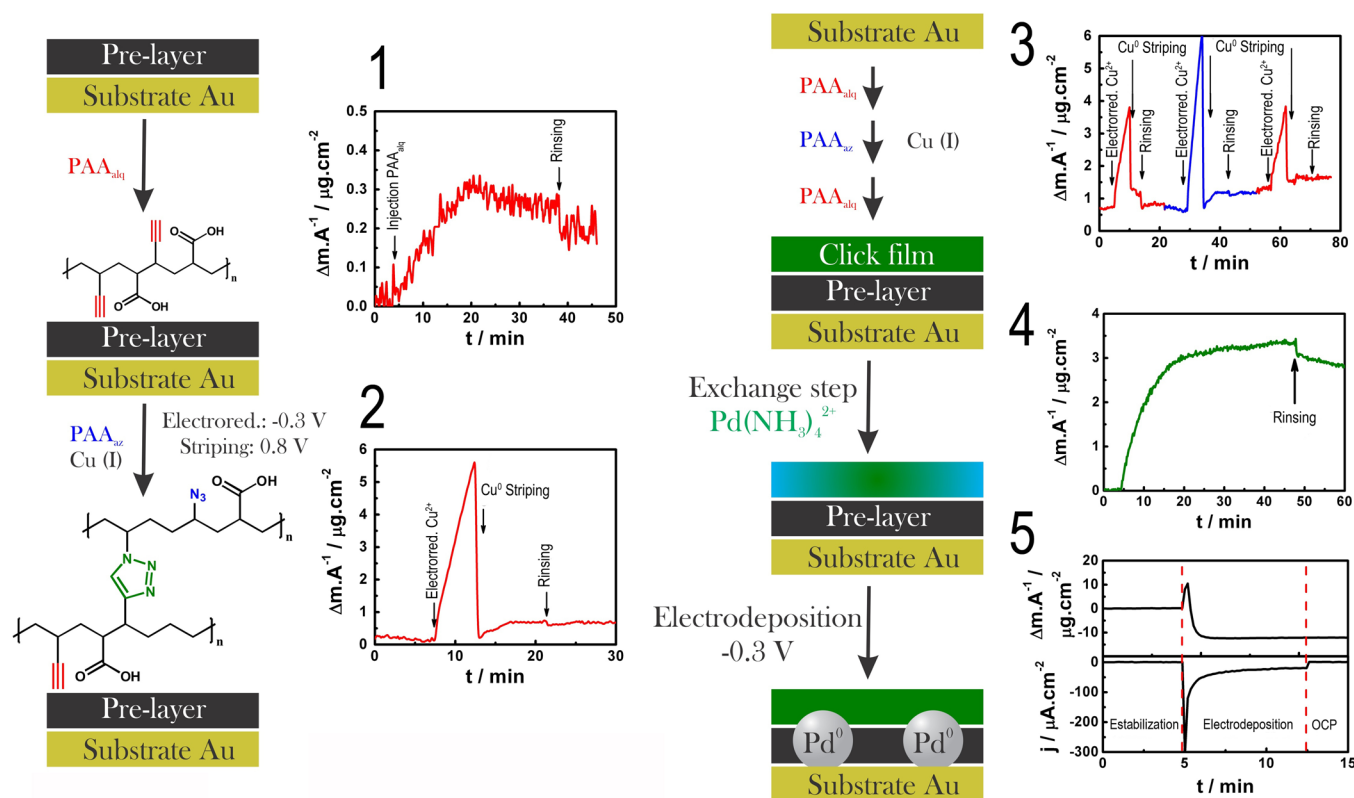
Recently, a novel strategy to build up single-component PAA multilayers with increased chemical and mechanical stability has been reported.¹³ The multilayers were successfully obtained by covalent cross-linking of PAA using the Sharpless “click chemistry” reaction,¹⁴ for example, 1,3-dipolar cycloaddition.¹⁵ The multilayer films can be grown by chemical¹⁶ or electrochemical^{10,17} reduction of Cu^{2+} to Cu^+ , which catalyzes the cycloaddition. The main advantages of the in situ production of the reaction catalysts Cu^+ are the controlled buildup of the multilayer film and the total activity of monovalent copper ions. The “electro-click chemistry”–LbL assembly tandem offers several significant advantages: (i) excellent physicochemical properties and extremely high stability, (ii) a defined maximum PAA ionization degree at pH 7,^{18,19} and (iii) a homogeneous distribution of functional groups in the direction perpendicular to the substrate.

Herein, we report the buildup of a single-component multilayer film comprising covalently bound PAA layers acting as a pure cationic exchange membrane that takes up $\text{Pd}(\text{NH}_3)_4^{3+}$ from the aqueous solution adjacent to the

Received: April 20, 2016

Revised: June 13, 2016

Scheme 1



polyelectrolyte and yields Pd NPs upon electrochemical reduction. During the process, each individual deposition and “electro-click reaction” step was monitored by quartz crystal microgravimetry, ellipsometry, and infrared spectroscopy techniques to determine the mass, thickness, and the exchange capacity of redox cations. Furthermore, we succeeded in performing the synthesis of Pd NPs by electrochemical reduction of the metal precursor $\text{Pd}(\text{NH}_3)_4^{3+}$ confined in the LbL film. To the best of the knowledge of the authors, this is the first disclosure of the LbL formation of NPs in PAA hydrogels using click chemistry reactions with good control over the film thickness.

EXPERIMENTAL METHODS

PAA (MW = 46 000) 10 wt % in water (CAS number 9003-01-4), propargylamine (CAS number 2450-71-7), poly(allylamine hydrochloride) (PAH) (MW = 56 000; CAS number 71550-12-4), cysteamine (CAS number 60-23-1), potassium tetrachloropalladate(II) (CAS number 10025-98-6), hexaammineruthenium(III) chloride (CAS number 14282-91-8), tetraamminepalladium(II) nitrate (CAS number 13601-08-6), sodium hydroxide (CAS number 1310-73-2), 2-bromoethylamine (CAS number 2576-47-8), sodium azide (CAS number 26628-22-8), *N*-methyl-2-pyrrolidone (NMP) (CAS number 872-50-4), *N,N'*-dicyclohexylcarbodiimide (CAS number 538-75-0), *N*-hydroxysuccinimide (CAS number 6066-82-6), and copper sulfate (CAS number 23254-43-5) were purchased from Sigma-Aldrich. Sulfuric and hydrochloric acids were supplied by Merck. All reagents were used as-received, and the solutions were prepared with deionized water (Milli Q, 18 MΩ·cm) with unbuffered solutions of pH approximately 5.5.

For the synthesis of 2-azidoethylamine, 1 g of 2-bromoethylamine was dissolved in 5 mL of water, and then the solution of sodium azide (3 equiv of the amine) was added to a round-bottom flask with vigorous stirring at 80 °C and refluxed for 15 h. **Caution:** It is well known that short carbon-chain azides are potentially explosive

substances, thus the evaporation of the solvent and temperature must be controlled very carefully.”

The reaction mixture was cooled down in an ice/salt bath (ca. −7 °C), and the reaction product was extracted three times with ethyl ether. The solvent was evaporated at 40 °C under vacuum and a viscous transparent liquid was obtained. For the PAA modification, 1 g of PAA was dissolved in 10 mL of NMP at 60 °C for 2 h and sonicated for 30 min. Under mechanical stirring, 2.8 g of *N,N'*-dicyclohexylcarbodiimide was added, and 5 min later, 1.5 g of *N*-hydroxysuccinimide in 10 mL of the same solvent was added to the reaction mixture. The solution was heated at 60 °C for 2 h and then filtered, discarding the solid urea as a by-product of the reaction. The solution was divided into two aliquots: 76 mg of propargylamine in NMP was added to the first one and 118 mg of 2-azidoethylamine in the same solvent was added to the second one. Both reaction mixtures were heated at the same temperature for 12 h, and then the contents were diluted with water and dialyzed against 0.5 M NaCl for 2 days and water for the following 5 days. The resulting polymers were characterized by NMR and FTIR spectroscopy (for details, see Figures S1 and S2). The integration analysis gave a substitution ratio of 15% for PAA_{alk}, whereas the modification with azide resulted in 12% of the total carboxylic acid groups being successfully functionalized (see Figure S3 for full NMR and integration). MestRe Nova software was used for the localization and integration of the NMR peaks.

NMR spectra were obtained using a Bruker Avance II 500 spectrometer (500 MHz, multinuclear), whereas IR spectra were taken using a Thermo Nicolet 8700 (Nicolet) spectrometer equipped with a custom-made external tabletop optical mount, an MCT-A detector (Nicolet), a photoelastic modulator (PM-90 with a II/Zs50 ZnSe 50 kHz optical head, Hinds Instruments), and a synchronous sampling demodulator (GWC Instruments) for PM-IRRAS experiments and transmission mode.

Electrochemical quartz crystal microbalance (EQCM): The quartz crystal resonator at 10 MHz was used as a quartz crystal microbalance (QCM) with a complex voltage divider to measure the resonant frequency and both components of the quartz crystal Butterworth–

Van Dyke equivalent circuit, which is described elsewhere.^{5,20} The crystals were mounted in the cells by means of viton O-ring seals, with only one face in contact with the electrolyte. The EQCM was used in situ to quantify (i) the polyelectrolyte mass uptake during the LbL adsorption onto a positively charged thiolated Au electrode and (ii) further metal complex exchange with the electrolyte within the multilayer film. Before the multilayer construction, the Au-coated quartz electrode was cleaned by repetitive potential cycles between 0 and 1.6 V in a 0.1 M H₂SO₄ solution at 1 V·s⁻¹, followed by 0.1 V·s⁻¹ scan before the adsorption of 1 mM cysteamine in ethanol.

The PAA_{alk}/PAA_{az} LbL multistep procedure has been described by Boulmedais et al.¹⁷ The concentration of all polymers was 0.83 g/L. The adsorption of polyelectrolytes was accomplished from solutions of pH 3.5 (both polymers and CuSO₄), whereas the Pd complex solutions were adjusted at pH 7 to obtain the maximum inclusion capacity, with stabilization and rinsing steps in the absence of the polyelectrolyte.

The film thickness of dry films in air was determined in a SENTECH (Berlin, Germany) variable angle rotating-analyzer automatic ellipsometer (vertical type, 2000 FT model), equipped with a 632 nm laser as a polarized light source. All the measurements were performed at an incidence angle of 70°. The gold electrode was horizontally mounted in a Teflon holder and aligned before each experiment. Ellipsometric parameters (Δ and Ψ) were collected in the operator-triggered mode after each adsorption step with the modified electrode surface in contact with air. The experimental data were fitted as described elsewhere⁵ taking into account a three-layer model: substrate, film, and air.

All electrochemical experiments were performed with an Autolab PGSTAT 30 potentiostat (Autolab, Ecochemie, Holland) with Nova 1.10 software. An Ag/AgCl (3 M KCl) electrode was used as a reference electrode, and a platinum gauze was used as the counter electrode.

The nanoscale images were taken using a Zeiss Supra 40 scanning electron microscope with an electron source accelerated at 10 keV to obtain the best contrast between the NPs and the substrate (resolution about 1.3 nm). The particle-counting was done with Image-Pro software, taking into account the average of at least three images.

RESULTS AND DISCUSSION

Scheme 1 depicts the strategy followed to build up Pd NPs utilizing an LbL nanostructured film using electro-click chemistry reactions: first, the Au surface was modified by adsorption of cysteamine to set up a positive charge on the surface. Subsequently, the negatively charged PAA_{alk} was electrostatically adsorbed from a 0.83 g/L aqueous solution, and the mass uptake time evolution is shown in **Figure S4A**. The second step in **Scheme 1** is the immersion of the modified surface in a new aqueous solution containing both 0.83 g/L PAA_{az} and 2 mM CuSO₄ while applying a potential step to -0.3 V to reduce Cu²⁺ to Cu⁺, which in turn acts as a catalyst for the electro-click reaction. This is followed by anodic stripping of the excess copper deposited on the Au substrate. In the third step (**Scheme 1**), after rinsing with water, we exchanged the 0.83 g/L PAA_{az} and 2 mM CuSO₄ with an aqueous solution containing 0.83 g/L PAA_{alk} and 2 mM CuSO₄ while applying -0.3 V again, followed by anodic stripping and rinsing. The last two steps in the alternate deposition of PAA_{alk} and PAA_{az} were repeated for a preset number of cycles (third step in **Scheme 1**).

Both the mass uptake and the ellipsometry film thickness increase linearly during the successive cycles, as shown in **Figure 1A,B**, respectively (ellipsometric angles are shown in **Figure S4B**). It should be noticed that in the absence of Cu²⁺ reduction to Cu⁺, less mass is observed. Therefore, the repetitive electro-click reaction over several steps leads to a

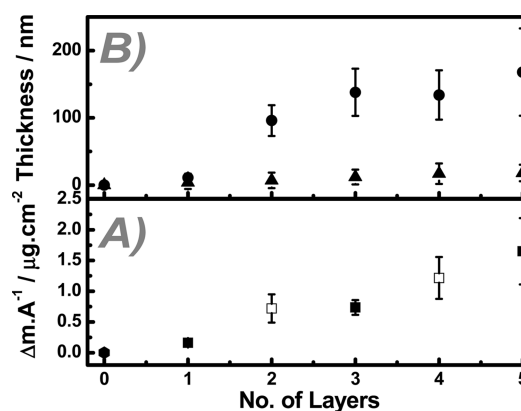


Figure 1. EQCM mass of ● PAA_{alk} and ○ PAA_{az} electrochemically deposit (A) and resulting ellipsometric thickness, ■ and □ respectively (B) for PAA_{alk}/PAA_{az} films as a function of the number of layers in the presence (solid circles) and absence (triangles) of CuSO₄ in the solution during electrochemical formation of catalyst Cu⁺ ion.

thicker film. Also, the electrodeposition of Cu simultaneously to the adsorption of PAA through the electro-click reaction is revealed by the anodic stripping current peak (shown in **Figure S4A**).

The difference between the masses at the final and initial stages corresponds to the PAA incorporated into the multilayer. A linear increment of the adsorbed polyelectrolytes up to five layers, with an average slope of 330 ng·cm⁻² per layer, has been observed.

Both PAA_{alk} and PAA_{az} are negatively charged polyelectrolytes, and therefore, the electro-click reaction is responsible for the film growth without surface charge overcompensation by the formation of polycation–polyanion pairs. The average thickness of 160 nm was found for five self-assembled layers, which is 10 times larger than that of a typical electrostatic film built with positively charged PAH and negatively charged PAA under the same solution pH conditions. The film thickness difference can be ascribed to the click reaction, which probably leads to a more open structure conformation by the repulsion of carboxylate groups in the PAA chains of successive layers and the absence of polycation–polyanion electrostatic attraction.

The spectroscopic evidence of the covalent film growth was obtained by the infrared measurement of the PAA_{alk} carboxylate groups and both azide and 1,2,3-triazole groups in the PAA_{az}. **Figure 2** shows PM-IRRAS spectra of films for increasing number of layers in the region of 1300–2400 cm⁻¹. A linear

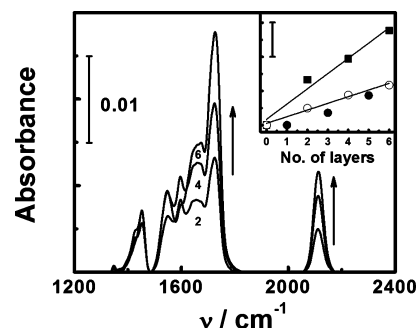


Figure 2. PM-IRRAS spectra of (PAA_{alk})_n(PAA_{az})_m films in air for 2, 4, and 6 deposited layers (indicated). Inset: Absorbance at 1727 (squares) and 2110 cm⁻¹ (open and closed circles) as a function of the number of layers.

growth of the 1727 cm^{-1} band assigned to $\text{C}=\text{O}$ stretching of the protonated form of carboxylic acids and a 2110 cm^{-1} band assigned to the overlap of $\text{N}=\text{N}$ and $\text{C}\equiv\text{C}$ stretching in the azide and alkyne is observed, with a higher molar absorption coefficient for the $\text{C}=\text{O}$ stretching band.

It is noted that when one PAA_{alk} layer is adsorbed by the electro-click reaction, the intensity of the 2110 cm^{-1} band decreases (inset in Figure 2, closed circles), indicating that a small fraction of azide groups are reacting with alkynes (see IR spectra of each deposited layer in the region of $\text{N}=\text{N}$ stretching in Figure S5). Also, in the absence of Cu^+ catalyst of the electro-click reaction, no film growth has been detected, and therefore, we conclude that the click reaction must have formed covalent bonds.

The linear growth in EQCM gravimetric, ellipsometric thickness, and spectroscopy is consistent with the findings reported by Caruso et al.¹³ and Boulmedais et al.¹⁷ However, the absolute value of the film thickness is higher probably because of the rinsing steps performed with Milli Q water at pH a bit lower than neutral after each layer adsorption.

The fourth step in Scheme 1 shows the incorporation of positively charged metal complexes, namely, hexaammineruthenium(III) and tetraaminopalladium(II) as a redox probe and a source of Pd NPs, respectively. At the end of the adsorption process during rinsing with water, a small decrease in loosely bound molecules was observed in both covalent $(\text{PAA}_{\text{alk}})_n(\text{PAA}_{\text{az}})_n$ and electrostatic $(\text{PAH})_n(\text{PAA})_m$ films. Cyclic voltammetry experiments with both $\text{Ru}(\text{NH}_3)_6^{3+/2+}$ and $\text{Fe}(\text{CN})_6^{3-/4-}$ have shown amphoteric exchange in $(\text{PAH})_n(\text{PAA})_m$ films, unlike covalent $(\text{PAA}_{\text{alk}})_n(\text{PAA}_{\text{az}})_n$ films, which behave only as a cationic exchanger.²¹ The $\text{Ru}(\text{NH}_3)_6^{3+}$ probes the ion-exchange capacity of the film for an electroactive positively charged redox active molecule and the electrical connectivity, and assesses the population of the ruthenium complex ion in the film. Figure 3

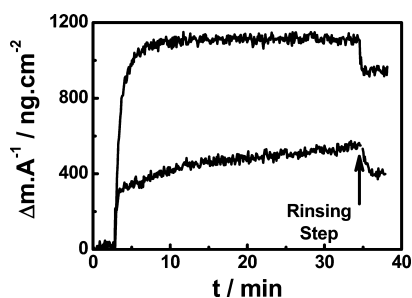


Figure 3. EQCM mass uptake during the exchange of $\text{Ru}(\text{NH}_3)_6^{3+}$ by $\text{Au}/(\text{PAA}_{\text{alk}})_3(\text{PAA}_{\text{az}})_2$ multilayer (upper curve) and $\text{Au}/(\text{PAA})_3(\text{PAH})_2$ (lower curve) films with the rinsing step at the end of redox cation exchange.

shows a comparison of the $\text{Ru}(\text{NH}_3)_6^{3+}$ mass uptake by the “electro-click” covalently bound multilayer nanoreactor and by the electrostatically self-assembled nanoreactor comprising PAA anion and PAH cation. The former film exchanges almost twice as much $\text{Ru}(\text{NH}_3)_6^{3+}$ as the latter because a larger fraction of carboxylates are available to bind cations as a result of the absence of polycation–polyanion pairs in the “click reaction” film. It has also been noticed that only 12–15% of the carboxylate groups in the PAA have been derivatized by alkyne and azide.

Next, Figure 4 depicts that the redox switch of both films during linear scan voltammetry with larger redox charge of the

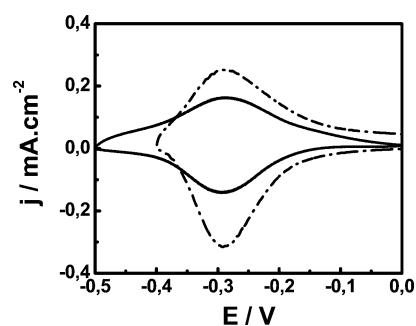


Figure 4. Cyclic voltammogram of $\text{Ru}(\text{NH}_3)_6^{3+}$ exchanged with $\text{Au}/(\text{PAA}_{\text{alk}})_3(\text{PAA}_{\text{az}})_2$ (dotted–dashed line) and $\text{Au}/(\text{PAA})_3(\text{PAH})_2$ (continuous line) in 0.1 M KNO_3 at $0.1\text{ V}\cdot\text{s}^{-1}$.

$\text{Ru}(\text{NH}_3)_6^{3+/2+}$ redox couple for the click reaction film is in good agreement with the difference in the mass uptake of redox cations exchanged by both films. Although for the $(\text{PAA}_{\text{alk}})_n(\text{PAA}_{\text{az}})_n$ multilayer, the mass uptake from the $\text{Ru}(\text{NH}_3)_6^{2+}$ solution reaches $950\text{ ng}\cdot\text{cm}^{-2}$, the electrostatically self-assembled PAA–PAH films reach only $400\text{ ng}\cdot\text{cm}^{-2}$, and cyclic voltammetry shows, respectively, 113 and $60\text{ ng}\cdot\text{cm}^{-2}$ of the redox active material within the experimental time scale. Thus, not all of the redox complexes in both multilayer films are directly accessible in the electrochemical experiment but almost the same ratio of ion-exchanged $\text{Ru}(\text{NH}_3)_6^{2+}$ complexes in both films is observed by both experimental techniques. The outermost layers in the films are out of reach of tunneling electrons from the underlying electrode, as has also been shown using XPS analysis in $(\text{PAH})_n(\text{PAA})_m$ with entrapped $\text{Pd}(\text{NH}_3)_4^{3+}$ ions.¹¹

As we have shown that PAA films self-assembled by the click reaction can efficiently exchange redox cations like $\text{Ru}(\text{NH}_3)_6^{3+}$, now we will focus on the ability of these multilayer films to exchange $\text{Pd}(\text{NH}_3)_4^{2+}$ with further electrochemical reduction to produce Pd NPs within the nanoreactor structure and investigate the shape and size of the resulting metal NPs.

Figure 5 shows a comparison of the mass uptake during the ion exchange of $\text{Pd}(\text{NH}_3)_4^{2+}$ in the electrolyte solution between

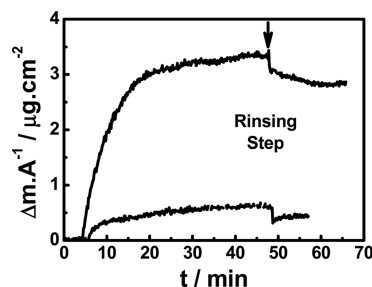


Figure 5. EQCM mass uptake during the exchange of $\text{Pd}(\text{NH}_3)_4^{2+}$ by $\text{Au}/(\text{PAA}_{\text{alk}})_3(\text{PAA}_{\text{az}})_2$ multilayer (upper curve) and $\text{Au}/(\text{PAA})_3(\text{PAH})_2$ (lower curve) films with the rinsing step at the end of redox cation exchange.

the film formed by the click reaction with excess of carboxylate in the PAA backbone and the electrostatically self-assembled PAA/PAH, $\text{Au}-\text{PAA}_3-\text{PAH}_2$ film in which most of the carboxylates and amines are forming polycation–polyanion pairs. The mass increase during the exchange of $\text{Pd}(\text{NH}_3)_4^{2+}$ is more than six times larger for the click reaction film than that for the electrostatically self-assembled film. Again, a small loss

in mass is observed in both films during the rinsing step with water.

Although in the electrostatically self-assembled film, the exchange of $\text{Ru}(\text{NH}_3)_6^{2+}$ or $\text{Pd}(\text{NH}_3)_4^{2+}$ occurs at the expense of breaking polyanion–polycation pairs, the excess of carboxylate groups in the click reaction film results in redox cation exchange by displacing Na^+ cations in the film, a process favorable with respect to entropy.

The fifth step in Scheme 1 is the electrochemical reduction of $\text{Pd}(\text{NH}_3)_4^{2+}$ entrapped in the multilayer film to yield Pd NPs. Figure 6 shows the electrochemical reduction of $\text{Pd}(\text{NH}_3)_4^{3+}$

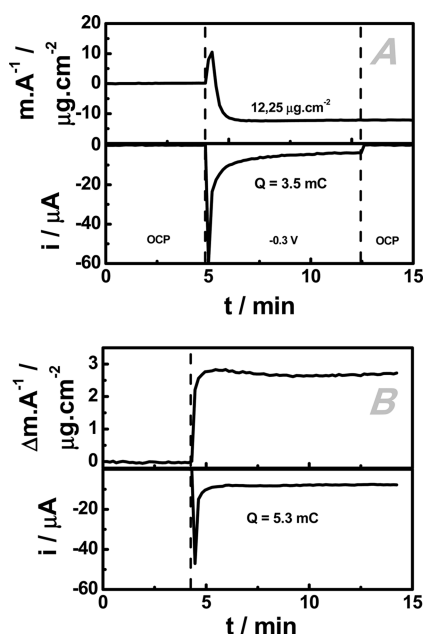
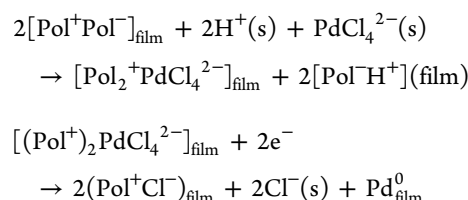


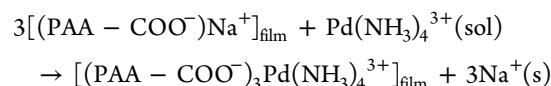
Figure 6. Chronoamperometry and simultaneous EQCM mass transient during the electrochemical reduction of $\text{Pd}(\text{NH}_3)_4^{2+}$ on $\text{Au}/(\text{PAA}_{\text{alk}})_3(\text{PAA}_{\text{az}})_2$ (A) and $\text{Au}/(\text{PAA})_3(\text{PAH})_2$ (B).

ions to form Pd NPs. Although the mass of the $\text{Au}/(\text{PAA}_{\text{alk}})_3(\text{PAA}_{\text{az}})_2$ multilayer film initially increases up to $10 \mu\text{g}\cdot\text{cm}^{-2}$ for a short period of time (20 s) and then decreases to the same value until a plateau is attained at longer times, the mass of the electrostatically self-assembled $\text{Au}/(\text{PAA})_3(\text{PAH})_2$ film reaches a constant value of $2.7 \mu\text{g}\cdot\text{cm}^{-2}$ after the potential step reduction is applied, experiencing similar currents for the NP formation/hydrogen evolution processes. Thus, EQCM electrogravimetry has shown different mechanisms for both types of films. For the former, an increase in the initial mass is indicative of the uptake of anions (Na^+ in this case), followed by a decrease in the mass for longer times because four NH_3 molecules leave the film for each Pd atom being reduced (Figure 6A), unlike the latter where only a small increase in mass is apparent during the formation of Pd NPs. It is worth noting that ions within multilayers can be exchanged with a different solvation sphere, which would explain the loss of the initial mass.

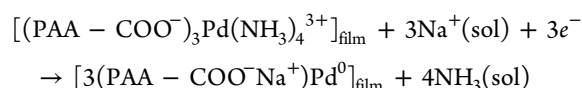
For electrostatically self-assembled positively charged PAH and negatively charged PAA, the ion exchange in Pd complexes and further electrochemical reduction to yield Pd NPs can be schematically represented by the stoichiometry equations.



Therefore, the small increase in the mass should arise from the solvent intake because of the change in the film volume. On the other hand, for the click reaction 1,2,3-triazole covalently bound PAA films, these processes can be represented, respectively, by the reactions



and



with an initial mass increase by the uptake of Na^+ compensating carboxylate charges, followed by the slow release of ammonia into the solution.

Unlike the as-prepared electrostatically self-assembled $(\text{PAH})_n(\text{PAA})_m$ multilayers that are reluctant amphoteric ion exchangers,³ the covalently bound PAA multilayer films are net cation exchangers. It is also observed that in the electrostatically formed film, intrinsic polycation–polyanion pairs are broken during the exchange of PdCl_4^{2-} with the electrolyte, whereas click reaction films do not have structural polycation–polyanion pairs and the exchange of $\text{Pd}(\text{NH}_3)_4^{3+}$ with the electrolyte is through extrinsic small cations with the cation exchanger PAA film.

During the electrochemical reduction step that yields the Pd NPs, the different gravimetric behaviors observed for click reaction films are the initial uptake of soluble cations to compensate the charge of the film carboxylate groups and the subsequent slow release of four NH_3 molecules per atom of Pd being reduced in the NP.

The resulting Pd NPs have also been characterized by cyclic voltammetry and scanning electron microscopy (SEM). Figure 7 shows a comparison of the electrochemistry of Pd NPs formed by the click reaction method and electrostatic self-assembly of PAA and PAH using cyclic voltammetry. The oxidation of Pd and reduction of PdO on the Pd NP surface are

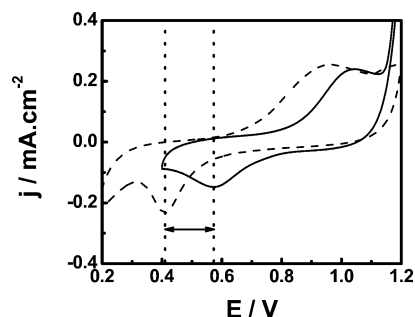


Figure 7. Cyclic voltammograms of Pd NPs formed by electrochemical reduction of $\text{Pd}(\text{NH}_3)_4^{2+}$ on $\text{Au}/(\text{PAA}_{\text{alk}})_3(\text{PAA}_{\text{az}})_2$ (dashed line) and $\text{Au}/(\text{PAA})_3(\text{PAH})_2$ (continuous line) in a 0.1 M H_2SO_4 solution at $0.1 \text{ V}\cdot\text{s}^{-1}$.

clearly seen in both cases (see Figure S6 for the cyclic voltammetry of $\text{Au}/(\text{PAA}_{\text{alk}})_3(\text{PAA}_{\text{az}})_2$ in the absence of the Pd precursor).

However, the difference in the PdO reduction peak potentials can be observed. For the click reaction film, PdO reduction takes place at the same potential as that on clean Pd metal electrodes, whereas for the electrostatically self-assembled film, the reduction is more irreversible with a 0.20 V shift in the peak potential. This shift in the PdO reduction peak potential has been observed previously and was ascribed to the strong adsorption of NH_2 on Pd NPs.²² In the click reaction film, on the other hand, there are no NH_2 groups attached to the polymer backbone to produce this effect. The electrochemically active areas of the metal NPs were estimated from the PdO reduction peak charge, assuming that one monolayer of PdO corresponds to $420 \mu\text{C cm}^{-2}$.

The size and shape distribution of the Pd electrodeposits created by applying the constant potential reduction step has been studied by SEM, as shown in Figure 8. Examination by

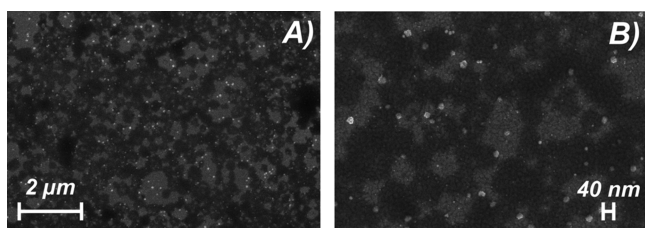


Figure 8. SEM images of the Pd NPs deposited on $\text{Au}/(\text{PAA}_{\text{alk}})_3(\text{PAA}_{\text{az}})_2$ by electrochemical reduction of $\text{Pd}(\text{NH}_3)_4^{3+}$ at -0.3 V at lower (A) and higher (B) magnifications.

SEM shows that Pd NPs formed on the electrode surface (Figure 8) are quasi-spherical NPs, with an average diameter of $50 \pm 8 \text{ nm}$ including 1077 NPs (see histogram in Figure S7), and are homogeneously distributed over the electrode surface.

In contrast to our previous work with the electrostatically self-assembled PAA–PAH film, we have obtained NPs with a typical diameter of 9 nm through the incorporation of a negatively charged Pd complex.²² Therefore, the nature of the multilayer matrix defines not only the ion exchange capacity but also controls the size of the NPs formed within the supramolecular structure by the volume available for the Pd NPs to nucleate and grow upon electrochemical reduction.

CONCLUSIONS

We have formed Pd NPs by electrochemical reduction of $\text{Pd}(\text{NH}_3)_4^{2+}$ ions entrapped in PAA multilayer films grown by the Sharpless click reaction of alkyne and azide groups covalently bound to the PAA. Unlike the electrostatically self-assembled PAA and PAH multilayers, which previously have been used as nanoreactors to form Pd NPs, in the 1,2,3-triazole covalently bound PAA films, the carboxylate groups do not form polyanion–polycation pairs, which defines their distinctive properties that these films behave as cation exchange membranes because only polyanions form the film structure. Also, the LbL films produced by the click reaction have a larger cation exchange capacity than electrostatically self-assembled polyelectrolyte films to take up redox ions such as $\text{Pd}(\text{NH}_3)_4^{3+}$, which yield Pd NPs upon electrochemical reduction.

The covalently bound films exhibit a more open structure than those of electrostatically LbL films probably because of the

repulsion of carboxylate groups and the lack of attraction between carboxylate and protonated amines in the electrostatic LbL films.

The size of the Pd NPs formed within the click reaction-bound $\text{Au}/(\text{PAA}_{\text{alk}})_3(\text{PAA}_{\text{az}})_2$ multilayer films, that is, 50 nm, is larger than that of similar Pd NPs formed in the electrostatically bound $\text{Au}/(\text{PAA})_3(\text{PAH})_2$ film nanoreactors, that is, 9 nm, under similar conditions. A larger mass of entrapped $\text{Pd}(\text{NH}_3)_4^{3+}$ and a more open structure of the covalently bound multilayers result in a larger NP size. Cyclic voltammetry of the resulting Pd NPs in a 0.1 M H_2SO_4 solution at 0.1 V s^{-1} shows the PdO reduction peak at the same value as that on a clean Pd surface unlike the NPs formed in the electrostatically bound $\text{Au}/(\text{PAA})_3(\text{PAH})_2$ nanoreactors with a 0.2 V shift in the cathodic direction, most probably because of the strong adsorption of amino groups on the Pd NP surfaces. This is particularly relevant to electrocatalysis by the Pd NPs.

During the electrochemical reduction of $\text{Pd}(\text{NH}_3)_4^{3+}$ ions to form Pd NPs, EQCM electrogravimetry has shown different mechanisms for both types of films: click reaction-bound $\text{Au}/(\text{PAA}_{\text{alk}})_3(\text{PAA}_{\text{az}})_2$ multilayer and the electrostatically bound $\text{Au}/(\text{PAA})_3(\text{PAH})_2$ films.

Here, we presented a unique application of polyacrylic gels previously reported as cation exchangers to form larger Pd NPs electrically connected to the substrate. Also, the controllable size of NPs, substrate-addressed, and their electrochemical activity close to the bulk material are the keys for a more suitable electrocatalyst in organic electrosynthesis, hydrogen production, and fuel cells because they minimize the amount of the noble material used in the deposition of the catalytic centers and the similarity of their electrochemical behavior compared to the massive material.

ASSOCIATED CONTENT

Supporting Information

The Supporting Information is available free of charge on the ACS Publications website at DOI: 10.1021/acs.langmuir.6b01519.

Synthesis 2-azidoethylamine, PAA modification, molecular structures of PAA, PAA_{alk} and PAA_{az} , PM-IRRAS spectra of $(\text{PAA}_{\text{alk}})_n(\text{PAA}_{\text{az}})_m$ films, cyclic voltammogram $\text{Au}/(\text{PAA}_{\text{alk}})_3(\text{PAA}_{\text{az}})_2$, NMR and FTIR spectra of PAA, PAA_{alk} , and PAA_{az} , and histogram of nanoparticle diameters (PDF)

AUTHOR INFORMATION

Corresponding Author

*E-mail: calvo@qi.fcen.uba.ar. Phone: 0054-1145763380.

Notes

The authors declare no competing financial interest.

ACKNOWLEDGMENTS

M.V. acknowledges a Ph.D. training fellowship from CONICET. The authors acknowledge the financial support from the University of Buenos Aires, CONICET, and ANCyPT grants PICT 2037/2008 and PICT 1452/2012.

REFERENCES

- (1) Decher, G.; Schlenoff, B. J. *Multilayer Thin Films*; Wiley-VCH: Weinheim, 2003.
- (2) Decher, G. Fuzzy Nanoassemblies: Toward Layered Polymeric Multicomposites. *Science* 1997, 277, 1232–1237.

- (3) Bucur, C. B.; Sui, Z.; Schlenoff, J. B. Ideal mixing in polyelectrolyte complexes and multilayers: Entropy driven assembly. *J. Am. Chem. Soc.* **2006**, *128*, 13690–13691.
- (4) Tagliazucchi, M.; Calvo, E. J. Electrochemically Active Polyelectrolyte-Modified Electrodes. In *Chemically Modified Electrodes*; Alkire, R. C., Kolb, D. M., Lipkowsky, J., Ross, P. N., Eds.; Wiley-VCH: Weinheim, 2009; Vol. 11, pp 57–115.
- (5) Forzani, E. S.; Otero, M.; Pérez, M. A.; Teijelo, M. L.; Calvo, E. J. The Structure of Layer-by-Layer Self-Assembled Glucose Oxidase and Os(Bpy)₂ClPyCH₂NH–Poly(allylamine) Multilayers: Ellipsometric and Quartz Crystal Microbalance Studies. *Langmuir* **2002**, *18*, 4020–4029.
- (6) Joly, S.; Kane, R.; Radzilowski, L.; Wang, T.; Wu, A.; Cohen, R. E.; Thomas, E. L.; Rubner, M. F. Multilayer Nanoreactors for Metallic and Semiconducting Particles. *Langmuir* **2000**, *16*, 1354–1359.
- (7) Wang, T. C.; Rubner, M. F.; Cohen, R. E. Polyelectrolyte Multilayer Nanoreactors for Preparing Silver Nanoparticle Composites: Controlling Metal Concentration and Nanoparticle Size. *Langmuir* **2002**, *18*, 3370–3375.
- (8) Kidambi, S.; Bruening, M. L. Multilayered Polyelectrolyte Films Containing Palladium Nanoparticles: Synthesis, Characterization, and Application in Selective Hydrogenation. *Chem. Mater.* **2005**, *17*, 301–307.
- (9) Kinnane, C. R.; Such, G. K.; Caruso, F. Tuning the Properties of Layer-by-Layer Assembled Poly(acrylic acid) Click Films and Capsules. *Macromolecules* **2011**, *44*, 1194–1202.
- (10) Bhattacharjee, S.; Dotzauer, D. M.; Bruening, M. L. Selectivity as a Function of Nanoparticle Size in the Catalytic Hydrogenation of Unsaturated Alcohols. *J. Am. Chem. Soc.* **2009**, *131*, 3601–3610.
- (11) Vago, M.; Tagliazucchi, M.; Williams, F. J.; Calvo, E. J. Electrodeposition of a palladium nanocatalyst by ion confinement in polyelectrolyte multilayers. *Chem. Commun.* **2008**, 5746–5748.
- (12) Villalba, M.; Bossi, M. L.; Calvo, E. J. Selective electrocatalytic hydrogenation using palladium nanoparticles electrochemically formed in layer-by-layer multilayer films. *Phys. Chem. Chem. Phys.* **2015**, *17*, 10086–10092.
- (13) Such, G. K.; Quinn, J. F.; Quinn, A.; Tjijto, E.; Caruso, F. Assembly of ultrathin polymer multilayer films by click chemistry. *J. Am. Chem. Soc.* **2006**, *128*, 9318–9319.
- (14) Jierry, L.; Ben Ameer, N.; Thomann, J.-S.; Frisch, B.; Gonthier, E.; Voegel, J.-C.; Senger, B.; Decher, G.; Felix, O.; Schaaf, P.; Mesini, P.; Boulmedais, F. Influence of Cu(I)-Alkyne π -Complex Charge on the Step-by-Step Film Buildup through Sharpless Click Reaction. *Macromolecules* **2010**, *43*, 3994–3997.
- (15) Bock, V. D.; Hiemstra, H.; van Maarseveen, J. H. Cu I-Catalyzed Alkyne-Azide “Click” Cycloadditions from a Mechanistic and Synthetic Perspective. *Eur. J. Org. Chem.* **2006**, 2006, 51–68.
- (16) El Haitami, A. E.; Thomann, J.-S.; Jierry, L.; Parat, A.; Voegel, J.-C.; Schaaf, P.; Senger, B.; Boulmedais, F.; Frisch, B. Covalent layer-by-layer assemblies of polyelectrolytes and homobifunctional spacers. *Langmuir* **2010**, *26*, 12351–12357.
- (17) Rydzek, G.; Thomann, J.-S.; Ben Ameer, N.; Jierry, L.; Mésini, P.; Ponche, A.; Contal, C.; El Haitami, A. E.; Voegel, J.-C.; Senger, B.; Schaaf, P.; Frisch, B.; Boulmedais, F. Polymer multilayer films obtained by electrochemically catalyzed click chemistry. *Langmuir* **2010**, *26*, 2816–2824.
- (18) Rydzek, G.; Polavarapu, P.; Rios, C.; Tisserant, J.-N.; Voegel, J.-C.; Senger, B.; Lavalle, P.; Frisch, B.; Schaaf, P.; Boulmedais, F.; Jierry, L. Morphogen-driven self-construction of covalent films built from polyelectrolytes and homobifunctional spacers: buildup and pH response. *Soft Matter* **2012**, *8*, 10336–10343.
- (19) Choi, J.; Rubner, M. F. Influence of the Degree of Ionization on Weak Polyelectrolyte Multilayer Assembly. *Macromolecules* **2005**, *38*, 116–124.
- (20) Etchenique, R. A.; Calvo, E. J. Electrochemical quartz crystal impedance study of redox hydrogel mediators for amperometric enzyme electrodes. *Anal. Chem.* **1997**, *69*, 4833–4841.
- (21) Villalba, M. *Metal Ion Confinement in Self-Assembled Multilayers for the Formation of Nanoparticles for Electrocatalytic Hydrogenation*; Doctoral, Buenos Aires University: Buenos Aires, 2015.
- (22) Villalba, M.; Bossi, M. L.; Calvo, E. J. Selective electrocatalytic hydrogenation using palladium nanoparticles electrochemically formed in layer-by-layer multilayer films. *Phys. Chem. Chem. Phys.* **2015**, *17*, 10086–10092.